



Substrate selection for heterotrophic bacterial growth in the sea



John R. Casey^{a,b,*}, Paul G. Falkowski^c, David M. Karl^{a,b}

^a Daniel K. Inouye Center for Microbial Oceanography: Research and Education, 1950 East-West Road, Honolulu, HI 96822, USA

^b School of Ocean and Earth Science and Technology, Department of Oceanography, University of Hawaii at Manoa, Honolulu, HI 96822, USA

^c Institute of Marine and Coastal Sciences and Department of Earth and Planetary Sciences, Rutgers University, New Brunswick, NJ 08901 USA

ARTICLE INFO

Article history:

Received 22 January 2015

Received in revised form 24 June 2015

Accepted 24 June 2015

Available online 29 July 2015

Keywords:

Substrate preference

¹⁴C respirometry

Dissolved organic matter turnover

Resource competition

Uptake kinetics

ABSTRACT

Growth of heterotrophic microbes requires the extraction of energy, electrons, carbon, and nutrients from a complex and dynamic reservoir of potential substrates. We employed a matrix of selected organic substrates with varying characteristics, and experimentally followed the kinetics of assimilation and respiration to explore the basic principles that govern selection and preferential use based on carbon, nitrogen, and energy content. We further competed these substrates in a combinatorial fashion to evaluate preferential substrate utilization in natural microbial assemblages. Several substrates displayed biphasic kinetic responses and variable respiration: assimilation ratios. Amino acids had the shortest turnover times and were taken up preferentially at ambient concentrations. We also identified a linear relationship between substrate uptake rates and affinity, suggesting that the microbial community optimizes the relative abundances of membrane transporters according to substrate demand. When competed against one another at saturating concentrations, substrate assimilation and respiration rates were enhanced or inhibited by up to two orders of magnitude, compared to competitor-free controls. Further, we describe an unexpected trend between the substrate energy density and turnover times, with more energetic, reduced carbon substrates turning over more slowly than more oxidized substrates.

© 2015 Elsevier B.V. All rights reserved.

1. Introduction

Microbial communities in the oligotrophic gyres are profoundly complex, both in terms of taxonomic diversity and metabolic potential, and interpretations of monoclonal laboratory cultures cannot easily be extended to the natural environment. Consequently, a qualitative, let alone quantitative, understanding of microbial community substrate preference is currently lacking. In the contest for resources, specialists and generalists inevitably compete with unique metabolic strategies. We hypothesize that individual microbes within the community optimize the utilization of growth-limiting resources. In the chronically inorganic nutrient depleted surface layer of the North Pacific Subtropical Gyre (NPSG), it might logically follow that dissolved organic nitrogen and/or phosphorus sources should be preferentially utilized by natural heterotrophic microbial communities (e.g., Casey et al., 2009). In this paper, we ask, “What are the basic principles that govern the selection of extracellular molecules for microbial growth?” We examine the hypothesis that heterotrophic microbial communities in the surface layer of a typical oligotrophic ocean gyre have evolved to preferentially utilize dissolved organic matter (DOM) substrates based on the hierarchy of energy density (KJ mol^{-1}), nitrogen mole fraction (mol N mol^{-1}), or carbon mole fraction (mol C mol^{-1}).

Substrates were chosen to represent a broad sampling of the bioavailable low molecular weight (LMW) organic substrate spectrum; four 6-carbon compounds with different energy densities (in terms of standard enthalpy of combustion; $\Delta H_c'$), three amino acids with different numbers of nitrogen atoms, and three carbohydrates with equal energy densities but different numbers of carbon atoms were selected as representatives of each class (Table 1). Gene products associated with the metabolism of all selected substrates were identified in Station ALOHA metagenome datasets (NCBI Accession: PRJNA13694, PRJNA29033, PRJNA16339) and in genomic DNA sequences of diverse bacteria and eukaryotes isolated from the NPSG surface waters, including alcohol and aldehyde dehydrogenases that are required for the metabolism of 1-hexanol. Other selected compounds (L-leucine, L-lysine, L-arginine, glyceraldehyde, D-ribose, D-mannose, citric acid, and hexanoic acid) are associated with central carbon metabolism, amino acid biosynthesis, and fatty acid synthesis/degradation pathways and therefore are readily metabolized by those organisms capable of transporting them. Individual substrate utilization and kinetics have been extensively investigated for numerous amino acid (e.g., Ayo et al., 2001; Kirchman and Hodson, 1986), sugar (e.g., Azam and Hodson, 1981; Nissen et al., 1984), nucleotide (e.g., Karl and Bailiff, 1989), and organic acid (e.g., Kieber et al., 1989; Wright and Hobbie, 1966) compounds present in the environment. However a comparative approach with multiple substrates is quite rare (c.f., Mopper and Kieber, 1991; Donachie et al., 2001).

* Corresponding author.

E-mail address: jrcasey@hawaii.edu (J.R. Casey).

Table 1

Comparison of selected substrates. Carbon enthalpies of combustion (ΔH_c°) were calculated according to the Kharasch Equation (see [Methods](#)). Respiration quotients (RQ) were derived from balanced respiration equations.

Compound	ΔH_c° [KJ mol C ⁻¹]	RQ [mol CO ₂ : mol O ₂]	Nitrogen [N atoms]	Carbon [C atoms]
Citric acid	377	1	0	6
Hexanoic acid	600	1.33	0	6
1-Hexanol	667	2	0	6
Glyceraldehyde	486	1	0	3
D-Ribose	473	1	0	5
D-Mannose	483	1	0	6
L-Leucine	615	0.8	1	6
L-Lysine	633	0.86	2	6
L-Arginine	652	1.1	4	6

To evaluate substrate preference, the assimilation and respiration kinetics of each substrate were measured by radioisotope incubations of natural surface seawater at Station ALOHA. We further hypothesized that substrate uptake (as the sum of assimilation plus respiration) and subsequent metabolism (as the ratio of respiration to uptake) are influenced by the presence of competing substrates. To evaluate substrate competition, each radioisotope tracer was incubated in the presence of a saturating concentration of each of the other substrates. Apart from a thorough competition of amino acids against different peptides ([Kirchman and Hodson, 1984](#)), we are unaware of a competition experiment involving multiple substrate classes in natural marine microbial assemblages.

Collectively, our field measurements indicate that natural heterotrophic microbial communities select substrates based on their nitrogen content over their carbon or energy content. Our results also lead to a somewhat surprising conclusion that higher energy density substrates (1-hexanol and hexanoic acid) turn over more slowly than lower energy density substrates (D-mannose, glyceraldehyde, and citric acid).

2. Methods

2.1. Sample collection

The experiments were carried out onboard the *R/V Kilo Moana* at Station ALOHA (22°45'N, 158°W) in March 2014. Seawater samples from 25 m were collected in the dark from 12 l Niskin® bottles each night following a 2100 h cast, approximately 3 h after sunset. Samples were collected over the course of 11 days alongside numerous biological, chemical, and hydrographic measurements, including measurements of community respiration based on diel cycles of O₂/Ar ([Ferrón et al., 2015](#)) and in vivo electron transport chain activity ([Martínez-García et al., 2009](#)). Sample collections, preparations, and incubations were conducted in the dark or under low intensity red light and all glassware was cleaned following recommendations by [Fitzwater et al. \(1982\)](#) to minimize trace metals contamination (pre-combusted, acid-washed, 0.22 µm filtered distilled deionized water-rinsed), which have been shown to affect amino acid uptake rate determinations in natural seawater samples ([Ferguson and Sunda, 1984](#)). Incubations were conducted at night, typically for 8 h, to avoid extracellular production of newly synthesized photosynthate and to encourage constant uptake rates (e.g., [Carlucci et al., 1984](#)).

2.2. Reagents and Supplies

We evaluated 9 compounds: [1,5-¹⁴C]citric acid, [1-¹⁴C]hexanoic acid, [1-¹⁴C]hexanol, [U-¹⁴C]D-mannose, [U-¹⁴C]L-leucine, [U-¹⁴C]L-lysine, [U-¹⁴C]L-arginine, [U-¹⁴C]glyceraldehyde, and [1-¹⁴C]D-ribose (MP Biomedicals, LLC; American Radiolabeled Chemicals, Inc.; [Table 1](#)). Uniformly labeled substrates were chosen, where available, to minimize ambiguity in interpretations of respiration and

assimilation ([Hamilton and Austin, 1967](#)), but this is inconsequential to uptake rate determinations. Unlabeled compounds and the reagents β-phenylethylamine (PEA herein), sulfuric acid, and formaldehyde (37 wt.%) were purchased from Sigma Aldrich Co. Dilute stocks of labeled substrates were made up to 92.5 MBq l⁻¹ and specific activities were adjusted to 1.85 GBq mmol⁻¹ by the addition of unlabeled carrier, with the exception of 1-hexanol which was prepared to 18.5 MBq l⁻¹ at 0.37 GBq mmol⁻¹. 1-Hexanol solutions were always less than 577 µM, the solubility limit for 1-hexanol in seawater at 20 °C.

2.3. Sample preparation and incubation conditions

Samples (70 ml) for kinetic and competition incubations were transferred to either 70 or 125 ml glass serum bottles for assimilation and respiration measurements, respectively. Kinetic experiments were initiated by the addition of 9 concentrations of a labeled substrate (from 1 nM to 365 nM, spaced logarithmically), in triplicate (n = 486). Competition experiments were initiated by the addition of 32 nM of a labeled substrate in the presence of 2 µM of each unlabeled substrate competitor, in triplicate (n = 486). A single killed control (fixed at 4 °C for 1 h with 2% w/v formaldehyde) was used for each treatment (n = 162). Following addition of the radiolabeled substrate, assimilation bottles were crimped sealed without a headspace with Teflon® stoppers using aluminum caps. The respiration bottles were fitted with “sleeve-style” rubber stoppers pierced with center well cups containing a dry piece of fluted cellulose filter paper (Whatman®) in the headspace. All bottles were incubated upright in the dark for 8 to 10 h, submerged in a bath of circulating surface seawater to approximately maintain the 25 m collection depth temperature (24.0 ± 0.1 °C).

2.4. Assimilation

Incubations were terminated by gentle vacuum filtration (<70 mBar) onto nominal 0.3 µm pore size glass fiber filters (GF75, Sterlitech). Bottles, caps, and filter funnels were thoroughly rinsed with 0.2 µm filtered seawater (three rinses of approximately 20 ml each). Filters were transferred to 20 ml glass scintillation vials followed by a 10 ml addition of scintillation cocktail (UltimaGold LLT, Perkin Elmer). ¹⁴C activity was counted on a Perkin-Elmer 2910TR TriCarb liquid scintillation counter using the spectral index of an external standard for quench correction. Substrate retained on the glass fiber filters or adsorbed to cells was estimated with killed controls, which were prepared for each concentration of each substrate. Killed controls were incubated alongside live samples and processed identically.

2.5. Respiration

Incubations were terminated by soaking the filter paper in the cup with 150 µl PEA and then acidifying the sample by adding 4 ml of 4.5 N sulfuric acid through the gas-tight stopper. The acidified solution was allowed to passively distill for 48 h before removing the stoppers. This procedure changes the dissolved CO₂ solubility and leads to a flux of ¹⁴CO₂ first into the headspace, then into center well cups containing the PEA. Center well cups containing the filter paper were transferred to scintillation vials. 500 µl aliquots of the remaining volume of each sample were also transferred to scintillation vials (n = 486). ¹⁴C activity was quantified identically to the filters (see *Assimilation*). Activity other than ¹⁴CO₂ that was retained by the cup was estimated by equilibrating each substrate in 0.2 µm filtered seawater and processing identically to live samples. ¹⁴CO₂ trapping efficiency was estimated by processing a known quantity of H¹⁴CO₃⁻ added to 0.2 µm filtered seawater.

2.6. Data analysis

Filter samples (i.e., “assimilation”) were corrected by subtracting killed control activities and cup samples (respiration) were corrected

for cell-free incubation activities. Transient isotope effects affect apparent uptake rates due to mass-dependent kinetic isotope fractionation under isotopic disequilibrium; specific transporter fractionation factors differ widely between different enzyme-substrate systems, and the respiration to assimilation ratio influences the magnitude of this effect. However, substrate specific activities and added concentrations were sufficiently high so as to reduce this effect to well below the analytical standard error of the measurement (<5% standard error). Kinetic parameters (Table 2) were determined for assimilation (v_A), respiration (v_R), and uptake (v_U) of each substrate by non-linear least squares (NLS) optimizations for each of four potential kinetics models:

$$\text{Monophasic: } v = \frac{V_{\max}[S_A]}{K_M + [S_A]} \quad (1)$$

$$\text{Monophasic/Diffusive: } v = \frac{V_{\max}^{\text{fast}}[S_A]}{K_M^{\text{fast}} + [S_A]} + K_D[S_A] \quad (2)$$

$$\text{Biphasic: } v = \frac{V_{\max}^{\text{fast}}[S_A]}{K_M^{\text{fast}} + [S_A]} + \frac{V_{\max}^{\text{slow}}[S_A]}{K_M^{\text{slow}} + [S_A]} \quad (3)$$

$$\text{Multiphasic: } v = \begin{cases} V_{\max}^{\text{fast}} \frac{S_A}{K_M^{\text{fast}} + S_A} & \text{if } S_A \leq b \\ V_{\max}^{\text{fast}} \frac{b}{K_M^{\text{fast}} + b} + V_{\max}^{\text{slow}} \frac{S_A - b}{K_M^{\text{slow}} + S_A - b} & \text{if } S_A > b, \end{cases} \quad (4)$$

where S_A is the substrate concentration [nM], b is the transition concentration [nM], K_M [nM] and V_{\max} [nM h⁻¹] are the Michaelis–Menten-like half-saturation constant and maximal rate, K_D is a diffusive parameter, and v is the kinetic velocity. To account for systematic analytical variance, which varied as a function of S_A added, we weighted the cost function using standard errors. A sensitivity analysis of the initialization parameters resulted in derived kinetics parameters that were stable to within <1% over a ten-fold range of expected values (data not shown). Models (1–4) were selected using the minimal Akaike Information Criterion (AIC) using the log-likelihood of each NLS fit; the AIC model selection procedure rewards the goodness-of-fit of each model while penalizing overly complex models. Standard errors for K_M and V_{\max} values were propagated by the root sum of squares deviation. Specific affinities (not biomass normalized) were calculated as the initial slope of the fast (α_f^0) and slow (α_s^0) subsets. Competition experiments were processed similarly, except that rates were treated as a fold-change relative to an unamended control.

Community respiration estimates corresponding to the same casts based on ΔO_2 :Ar and electron transport activity measurements varied by 28% and 19% over the course of the sampling period, respectively (Ferrón et al., 2015). This day-to-day natural variability was not taken into account in our error analysis and potentially influenced V_{\max} estimates since our experiments were conducted over an 11 day period, however, both community respiration estimates could explain <1% of the variance in V_{\max} ($p = 0.936$).

Standard enthalpies of combustion were calculated for each substrate according to a simplification of the Kharasch equation (Kharasch, 1929):

$$\Delta H_C' = 200a_1 + 280a_2 + 220a_3 + 105a_4 + 60a_5 + 40a_6 - 20a_7$$

Table 2
Parameters used in this study.

Parameter	Description	Units
α_f^0	Substrate affinity of fast transport system (K_M/V_{\max})	h ⁻¹
α_s^0	Substrate affinity of slow transport system (K_M/V_{\max})	h ⁻¹
K_M	Michaelis–Menten half-saturation constant	nM
K_D	Rate of diffusion	h ⁻¹
S_A	Substrate added concentration	nM
S_n	Natural (ambient) substrate concentration	nM
v	Transport velocity	nM h ⁻¹
v_o	Initial velocity	nM h ⁻¹
v_R	Respiration rate	nM h ⁻¹
v_A	Assimilation rate	nM h ⁻¹
v_U	Uptake rate ($v_R + v_A$)	nM h ⁻¹
V_{\max}	Maximum velocity	nM h ⁻¹

where the coefficients are the average bond energies (kJ mol⁻¹) corresponding to the number of π bonds in aromatic compounds (a_1), non-aromatic double bonds (a_2), σ and C–H single bonds (a_3), C–N and N–H bonds (a_4), carbonyl groups (a_5), hydroxy (a_6), and carboxyl groups (a_7).

3. Results and discussion

3.1. Method evaluation

We evaluated the ¹⁴C-respirometry method for determining compound-specific assimilation and respiration rates in natural seawater incubations. We consistently found quantitative recovery to be 99.85 ± 1.98% (calculated as the sum of filter, cup, and remaining activity as a percentage of activity added) and low sample-sample variability (8.3 ± 1.9%; Fig. 1). Killed control activities were consistently <0.1% of activity added and consistently <15% of assimilation with the exception of [1-¹⁴C]D-ribose (45.5 ± 17.9% of assimilation), indicating low cell surface and glass fiber filter adsorption over the entire S_A range. The trapping efficiency of PEA soaked filter paper after acidifying a known quantity of H¹⁴CO₃⁻ was 98.99 ± 4.28%. When the same procedure was followed for 32 nM additions of each labeled substrate in 0.2 μ m filtered seawater, the absorption was 0.08 ± 0.04% of total radioactivity added, with the exception of [1-¹⁴C]hexanol which was 10.4%.

3.2. Substrate preference and kinetics

Assimilation, respiration, and uptake kinetics were biphasic or multiphasic within the range 1 nM to 364.5 nM of S_A for 7 of the 9 substrates tested with “breakpoints” (the transition between two transporter systems operating at different concentration ranges) between 20 nM and 90 nM of the S_A (Fig. 2, Table 3). No differences in breakpoint concentrations were found between assimilation, respiration, or uptake kinetics curves for a given substrate. Multiphasic kinetics in natural marine bacterial populations have been reported previously for the metabolism of glucose and mixed amino acids (Azam and Hodson, 1981; Nissen et al., 1984) and for ectoenzyme kinetics (Unanue et al., 1999). Artifacts associated with S_A and S_n concentration dependencies of K_M and multiphasic kinetics have been proposed to result from a diffusive model with a sub-unity slope resulting from different membrane permeabilities, intracellular substrate concentrations, and kinetic fractionation of the radiolabeled substrate uptake between species (Logan and Fleury, 1993). However it is highly unlikely that marine bacteria rely on concentration gradients alone for substrate uptake, especially since intracellular metabolite concentrations are frequently in the μ M to mM concentration range (e.g., Bennett et al., 2009); rather, it is much more likely a combination of multiple transporters (Button, 1993). Although the multiphasic model has been theoretically and experimentally described in a multitude of biological systems (Nissen and Nissen, 1983), we cannot discount the possibility that breakpoints were an artifact of de novo transporter synthesis during the course of the approximately 8 hour incubations. The remaining two substrates were not well described by the multiphasic or biphasic models; rather a monophasic model was selected for L-arginine kinetics and an additional diffusive term best fit the kinetics of L-lysine, according to our AIC model selection procedure.

v_R/v_U ratios, which are upper constraints on bacterial growth efficiencies (BGE) due to isotopic disequilibrium of intracellular metabolite pools during short incubations (King and Berman, 1984), were not constant over the concentration range of substrates tested (Fig. 3). Coefficients of variation (CV) of substrate v_R/v_U ratios ranged from 14 to 45% for glyceraldehyde to L-arginine, respectively. S_A dependencies of BGE are ignored in most bacterial production assays, including those based on [³H]L-leucine assimilation (CV = 28%), and will introduce ambiguity to their interpretations since ambient substrate concentrations are

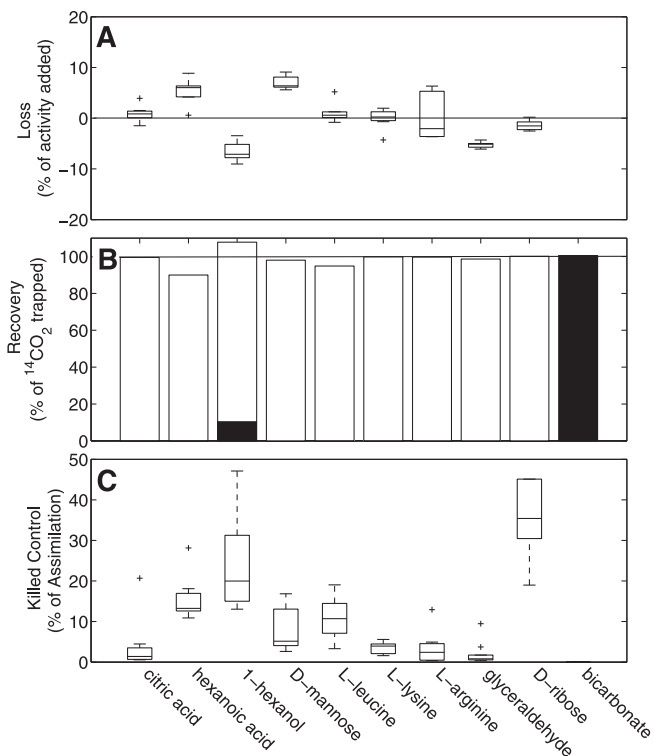


Fig. 1. Summary of performance of assimilation and respiration methods. A: “Box-and-Whiskers” plot of loss of radioisotope for each labeled substrate. Calculated for all samples ($n = 972$) as the percent of isotope added minus the sum of activities caught on the filter, trapped in the cup, and remaining in solution. B: Stacked bar plot of percent recovery of respirometry for each labeled substrate and $\text{Na}_2\text{H}^{14}\text{CO}_3$ (see Methods: Respiration; $n = 12$). Solid bars represent percent of added activity trapped in the cups; open bars represent percent of added activity remaining in solution. C: “Box-and-Whiskers” plot of killed control percent of assimilation for all kinetics samples ($n = 486$).

rarely measured prior to incubations and substrate is usually added at saturating concentrations (>20 nM; e.g., Church et al., 2004).

Because ambient substrate concentrations (S_n) were not measured, “tracer” substrate concentration additions, ideally $<10\%$ of S_n , were not necessarily achieved. We therefore approximate ambient substrate uptake rates as the initial velocity (v_0) at 1 nM S_A . With this proviso, amino acids were taken up at rates higher than other substrates tested. Another metric for substrate affinity, V_{max}/K_m (h^{-1}), was also found to be highest for the amino acids compared with other substrates. We found a linear relationship ($R^2 = 0.70$, slope = 0.85 ± 0.1 , $p = 0.0001$; Fig. 4) between the ambient substrate uptake rate and the substrate affinity, as expected for Michaelis–Menten kinetics at $S_A + S_n \ll K_m$. Agreement between ambient uptake rates and substrate affinities supports the hypothesis that microbial communities collectively optimize the scavenging of resources according to substrate availability and demand. Since K_m is an intrinsic property of transporter-substrate affinity, both the cell surface density of transporters and the distribution of transporters among different microbial community taxa are optimized for the exploitation of specific substrates. For example, amino acid transporters are likely common to a majority of microbial taxa, and may represent a larger fraction of outer membrane transporter proteins than e.g., fatty acid transporters, as was the case for coastal bacterioplankton (Poretsky et al., 2010).

Over the concentration range tested, we found that 1-hexanol was assimilated at rates comparable to other C_6 substrates. Marine microbes are known to use methanol as both a carbon and energy source, and several alcohol dehydrogenases are common to methylotrophic bacteria including the numerically dominant *Pelagibacter ubique* SAR11 (Sun et al., 2011). 1-Hexanol is dehydrogenated to hexanaldehyde and further to hexanoic acid and subsequently directed toward fatty acid synthesis or degradation pathways to regenerate acetyl-CoA. Perhaps since 1-hexanol is uniquely connected to hexanoic acid, ambient substrate uptake rates and substrate affinities were nearly identical for 1-hexanol and hexanoic acid, despite almost certainly depending on separate transporters due to differences in charge distribution. We

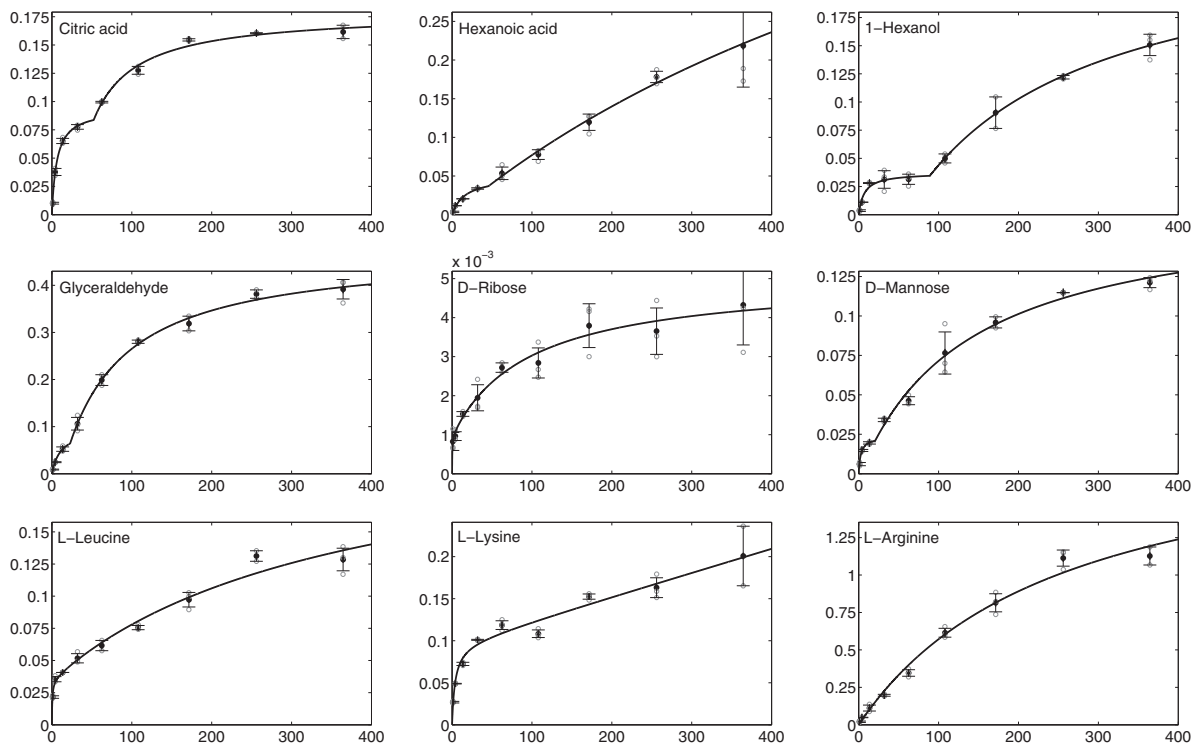


Fig. 2. Uptake kinetics ($v_U = v_A + v_R$) for all substrates. Mean values (filled symbols), standard deviations (error bars), data from triplicate samples (open symbols), and NLS regressions (lines) are shown for AIC selected models. Values for all transport systems are given in Table 3.

Table 3

Summary of uptake kinetics for each labeled substrate. Standard deviation reported in parentheses. NA- not applicable.

Substrate	Model	Breakpoint [nM]	V_{max} (Fast) [nM h ⁻¹]	K_m (Fast) [nM]	V_{max} (Slow) [nM h ⁻¹]	K_m (Slow) [nM]	R ²
Citric acid	Multiphasic	52.3	0.094 (0.003)	6.2 (0.6)	0.195 (0.003)	54.2 (3.2)	1.00
Hexanoic acid	Multiphasic	45.5	0.050 (0.004)	16.6 (2.4)	0.712 (0.150)	912.1 (109.1)	1.00
1-Hexanol	Multiphasic	89.1	0.037 (0.003)	6.9 (2.8)	0.218 (0.004)	243.8 (19.7)	1.00
Glyceraldehyde	Multiphasic	22.9	0.096 (0.010)	11.4 (1.5)	0.410 (0.021)	80.3 (8.7)	1.00
D-Ribose	Biphasic	NA	0.001 (7.1e ⁻⁵)	0.3 (0.1)	0.004 (2.2e ⁻⁴)	97.7 (11.5)	0.97
D-Mannose	Multiphasic	20.7	0.024 (0.001)	2.6 (0.4)	0.151 (0.001)	157.1 (15.1)	1.00
L-Leucine	Biphasic	NA	0.035 (0.001)	0.6 (0.2)	0.203 (0.015)	368.3 (57.1)	0.97
L-Lysine	Monophasic/Diffusive	NA	0.096 (0.003)	3.7 (0.6)	NA	$K_D = 0.0003$	0.97
L-Arginine	Monophasic	NA	2.028 (0.090)	255.1 (16.1)	NA	NA	0.99

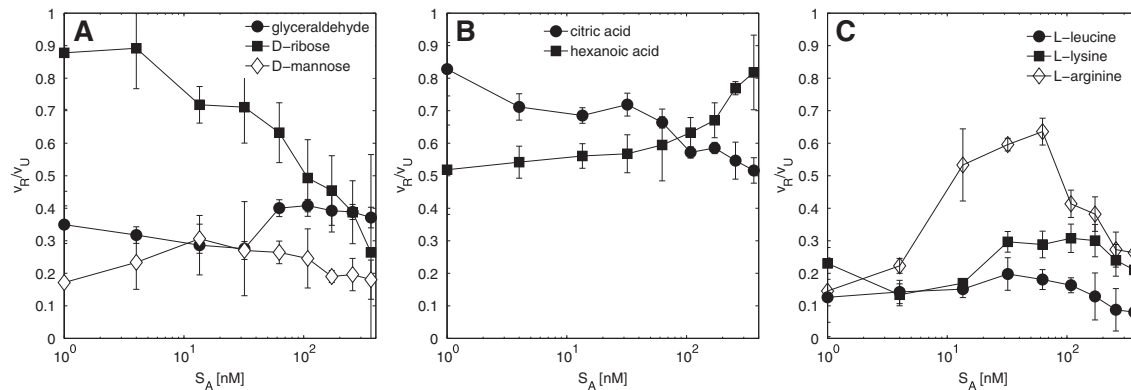


Fig. 3. Respiration: uptake (v_R/v_U) ratio for A: carbohydrates, B: carboxylic acids and C: amino acids over the S_A range (log scale). 1-Hexanol is not shown (see text).

estimated an upper limit on the concentration of 1-hexanol to be 7.0 ± 1.9 nM (Table 4), however there are no direct determinations for the ambient concentration of any primary alcohols other than methanol in seawater to compare. K_m and V_{max} values (Table 3) were comparable to methanol ($K_m = 9.3$ to 86 nM; $V_{max} = 1.0$ to 1.2 nM h⁻¹ in Dixon et al., 2011). 1-Hexanol respiration could not be determined due to a high sample blank, perhaps due to volatility and subsequent scavenging by PEA, though we are unaware of this reaction at room temperature. We suggest that future respirometry determinations of volatile and semi-volatile substrates use another trapping solvent (e.g., hyamine, a quaternary ammonium hydroxide).

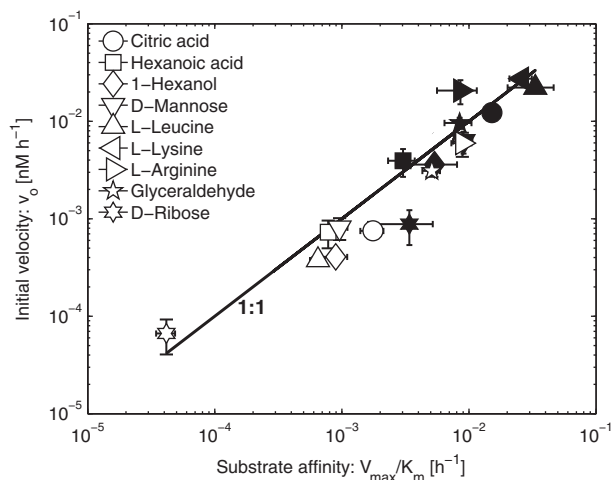


Fig. 4. “Ambient” substrate uptake rates (v_o) as a function of substrate affinity (a_R^0, a_S^0). Closed symbols correspond to fast uptake kinetics and open symbols correspond to slow uptake kinetics. Error bars represent one standard deviation for both variables. Values are plotted with the line of unity for reference.

D-Ribose was taken up at unexpectedly low rates and respiration was near the detection limit (3 times the standard deviation of v_R for each S_A concentration) resulting in poor confidence in kinetic constant estimates (3 out of 9 S_A concentrations with $p > 0.05$). This study is the first to report D-ribose uptake rates in natural seawater and the few direct concentration determinations available for the North Pacific suggest D-ribose is typically depleted (<5 mol%) in monomeric (MW < 200 Da), oligomeric (MW 200–4000 Da), and polymeric (MW > 4000 Da) fractions of total hydrolysable dissolved carbohydrates (Mopper et al., 1980; Sakugawa and Handa, 1983). Rather, D-ribose is likely present mostly as the sugar moiety of RNA and free or polymeric nucleotides, which are abundant both in cells and dissolved in seawater (Karl and Bailiff, 1989; Björkman and Karl, 2005). Pentosyltransferases, such as purine and pyrimidine nucleoside transferases are probably not active exoenzymes, otherwise we would expect an accumulation of dissolved D-ribose since nucleotide turnover times are relatively short (1–2 d; Björkman and Karl, 2005). Therefore, RNA and nucleotides must be transported prior to dissimilation (e.g., xanthine degradation

Table 4

Summary of turnover times and K_m (Fast) + S_n . Standard deviation reported in parentheses. D-Ribose not reported (see text).

Compound name	Turnover time [h]	$K_m + S_n$ [nM]
Citric acid	75.3 (9.2)	7.2 (0.4)
Hexanoic acid	277.2 (29.6)	12.9 (1.0)
1-Hexanol	981.3 (262.0)	7.0 (0.4)
Glyceraldehyde	109.0 (10.9)	9.7 (1.2)
D-Mannose	112.2 (13.4)	2.6 (0.1)
L-Leucine	44.1 (20.7)	2.4 (0.2)
L-Lysine	54.4 (15.1)	7.0 (0.4)
L-Arginine	74.6 (16.4)	38.1 (10.0)

pathway, purine catabolic pathways, pyrimidine catabolic pathways), or polymerization.

In contrast to D-ribose, the remaining carbon substrates (citric acid, glyceraldehyde, and D-mannose) were rapidly utilized. Of these, only D-mannose uptake has been previously reported in an aquatic ecosystem, albeit in a mesotrophic lake, with roughly comparable turnover times (20 to 170 h; Bunte and Simon, 1999). Citric acid v_R/v_U ratios (0.65 ± 0.10) were significantly higher ($p < e^{-6}$) than the other carbohydrates glyceraldehyde (0.35 ± 0.05) and D-mannose (0.23 ± 0.05). Glyceraldehyde and D-mannose v_R/v_U ratios were comparable to D-glucose in other marine environments (Williams, 1970; Williams and Yentsch, 1976). Although we expected high catabolism of citric acid due to its role as a tricarboxylic acid (TCA) cycle intermediate, high anabolic assimilation of carbohydrates suggests an unexpected prevalence of carbon storage by gluconeogenesis in marine bacteria inhabiting the NPSG. The disparity in the v_R/v_U ratio for glyceraldehyde and D-mannose further supports this hypothesis. Intermediates at the top of glycolysis (β -D-fructose-6-phosphate derived from D-mannose by hexokinase, M6P isomerase) are expected to show higher anabolism relative to bottom of glycolysis intermediates (2-phospho-D-glycerate or 3-phospho-D-glycerate derived from glyceraldehyde by glyceraldehyde dehydrogenase or triose kinase, respectively) under conditions where the oxidative pentose phosphate pathway flux is low.

Ambient uptake rates were similar ($p > 0.05$) between amino acids, however differences were observed in the substrate affinity, turnover, kinetic constants, and efficiencies of nitrogen assimilation. For example, the efficiency of nitrogen assimilation, expressed as the nitrogen assimilated as a molar fraction of the nitrogen added, increased in the order of nitrogen atoms per molecule (L-leucine (1) < L-lysine (2) < L-arginine (4)). Turnover times and K_m constants increased in the same order, while ambient substrate uptake rates were similar, suggesting transporter abundance (proportional to V_{max}) was predominantly responsible for the high uptake rates.

Among the carbohydrates, the number of carbon atoms was not a determinant in v_U , v_A , v_R , K_m , V_{max} , a_0^p , a_0^s , or turnover time. However, the turnover time was exponentially dependent on energy density (kJ mol C^{-1} ; Fig. 5). It is important to note that the carbon substrates exhibiting the most rapid turnover (citric acid, glyceraldehyde, and D-mannose) have potential energies, average degrees of reduction, and respiration quotients (RQ) closely matching those of microbial cell biomass (based on an average of *Escherichia coli* and *Saccharomyces cerevisiae*). Few compound-specific turnover time determinations are available for oligotrophic marine environments, still fewer with substrates representing a broad energy density range; however, the turnover dependence on substrate energy density appears to be consistent. For example, in an assessment of substrate-specific turnover times of 10 substrates in the Black Sea water column, L-ornithine was both the highest energy density substrate surveyed ($626 \text{ kJ mol C}^{-1}$) and had the longest turnover time (172 d; Mopper and Kieber, 1991). Long turnover times have been reported for other high energy density substrates; acetone ($607 \text{ kJ mol C}^{-1}$) turnover was estimated at 41–55 days in the oligotrophic gyres (Dixon et al., 2013), methanol ($700 \text{ kJ mol C}^{-1}$) turnover times were 7–33 days in the northeast Atlantic (Dixon et al., 2011), comparable to 1-hexanol turnover times (41 days). Methane ($880 \text{ kJ mol C}^{-1}$), the most reduced of all organic substrates, has been estimated to turn over between a few years and hundreds of years in the western North Pacific (Watanabe et al., 1995) and Sargasso Sea (Jones, 1991). The number of substrates surveyed in this and other studies are too few to formalize such a pattern; however, if this relationship holds for other labile LMW DOM substrates, it may be applied to the existing theoretical framework of ecological thermodynamics since both bacterial growth yield (mol C mol C^{-1} utilized) and bacterial C specific growth rate (mol C mol C^{-1} utilized d^{-1}) tend to increase as a linear and squared function, respectively, of the degree of reduction of substrate (Vallino et al., 1996). We observed no relationship between degree of reduction or energy density and v_R/v_U so the catabolic:

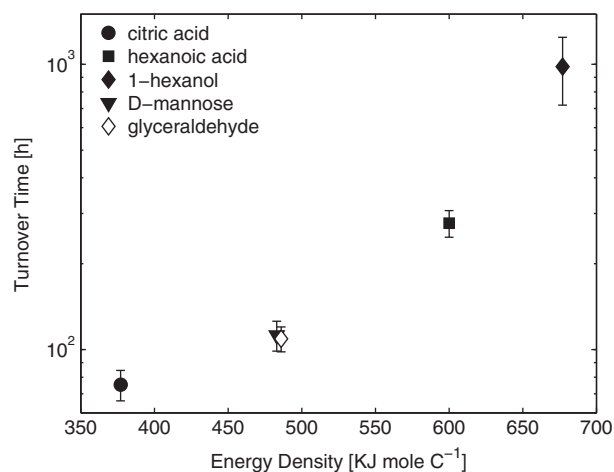


Fig. 5. Turnover time of carbon substrates as a function of energy density. Error bars represent one standard deviation of the mean.

anabolic ratio of individual substrates did not align with theoretical predictions of growth yield in our study site. Conversely, for a particular substrate as the sole carbon source for anoxygenic microbes, the thermodynamic efficiency for growth, defined as the product of the Gibbs energy of assimilation: chemical potential energy ratio and the growth rate: uptake rate ratio, is theoretically lower for reduced substrates (degree of reduction > 4) than oxidized substrates (Westerhoff, 1993). Correspondingly, the theoretical growth yield and the ratio of free enthalpy of catabolism to anabolism increases with degree of reduction of the substrate (Westerhoff et al., 1983). The degree of reduction of intermediate metabolites in the central carbon pathways of metabolism are reminiscent of this, since oxidized intermediates are associated with high flux central carbon metabolic pathways (TCA cycle, glycolysis, and the oxidative pentose phosphate pathway), while reduced metabolites (long-chain fatty acids and alcohols) are associated with linear biosynthetic and degradation pathways (e.g., fatty acid biosynthesis, β -oxidation) which turn over less rapidly. It is therefore plausible that the degree of reduction produces an imbalance in the production and consumption of LMW DOM substrates, resulting in the observed trend with turnover time. Even for specialists, a single carbon source is unlikely to support growth in the marine environment, so these generalizations are complicated by multiple and varying carbon sources.

3.3. Substrate competition

DOM composition is dynamic in the near-surface environment on both spatial and temporal scales; diel oscillations in photochemical production of organic matter, especially in the surface microlayer (e.g., Carlucci et al., 1984; Kieber et al., 1989; Zhou and Mopper, 1997), and diel oscillations in phytoplankton extracellular DOM production interact with diurnal mixing cycles to alter the DOM age and composition throughout the upper water column. The intention of the competition experiment was to broadly evaluate changes in substrate uptake rates in the presence of saturating concentrations of substrates that could aid in our interpretation of pairwise comparisons of kinetics experiments, in a combinatorial manner. Substrate utilization is constrained by one of two proteins: the membrane transporter (or porin), and a rate-limiting metabolic reaction. For marine bacterial genomes and metagenomes, adequate functional characterizations of membrane transporters are unavailable; transporters are often annotated by homology to no better than the family level. With neither the adequate identification nor the abundance of transporters known, the distinction between transporter rate-limitation and metabolic rate-limitation is unclear. Considering that a typical oligotrophic bacterium ($0.4 \mu\text{m}$ diameter) may have space for only 10^3 to 10^4 individual

membrane transporter proteins (based on approximate protein sizes, spacing, and surface area; Albe et al., 1990), and given the diversity of potential substrates and minimal genome sizes, it is likely that many transporters are of broad specificity and therefore subject to competitive inhibition. Ultimately, the competitor may act in a great many ways to affect a change in apparent uptake rates of the labeled substrates.

We observed complex interactions between many labeled substrates and their competitors, affecting significant changes in uptake rates and the fraction of uptake respired, spanning more than a factor of 20 and 7, respectively (Fig. 6). In general, competing substrates with similar chemical properties (e.g., L-lysine and L-arginine) and/or mutual metabolic pathways (e.g., hexanoic acid and 1-hexanol) were inhibitors of one another, while substrates of varied structure from disparate branches of the metabolic network affected assimilation and respiration changes in more complex ways. We highlight several of these interactions below; however, we stress that in all cases, inhibitive or enhanced rates and ratios are exaggerated relative to natural conditions due to the high concentration (2 μ M) of competitor added with each labeled substrate.

As might be expected, amino acids were potent inhibitors of other amino acids, with $50.0 \pm 0.2\%$, $72.7 \pm 1.2\%$, and $88.1 \pm 6.3\%$ inhibition of uptake for L-leucine, L-lysine, and L-arginine, respectively, regardless of which saturating amino acid competitor was used. This result, together with similarity in the breakpoint of high and low affinity transport systems between these three amino acids, suggests that a high-affinity but broad substrate-specificity amino acid transporter may be prevalent and rate-limiting. Alternatively, metabolic regulation of protein synthesis may be rate-limiting; Kirchman and Hodson (1984) used oligopeptides as surrogates to alter the intracellular amino acid pool size, based on the assumption that free and polymeric amino acids do not share transport systems. They attributed the oligopeptide inhibition of extracellular amino acid uptake to ‘buildup’ of intracellular amino acid pools and suggested the feedback indicates direct coupling between amino acid uptake and protein synthesis. In our competition experiment, amino acid competitors similarly affected the fraction of substrate uptake that was subsequently respired; L-leucine, L-lysine, and L-arginine v_R/v_U ratios

decreased by $53.4 \pm 1.5\%$, $53.8 \pm 14.1\%$, and $58.7 \pm 11.9\%$, respectively. Presumably, decreased v_R/v_U ratios are an indication of connectivity of amino acid pools; degradation of the competitor amino acid to ammonia and subsequent de novo protein synthesis would result in enhanced assimilation of the labeled amino acid. L-leucine also inhibited the uptake of all other substrates, with the curious exception of an increase in both hexanoic acid and 1-hexanol respiration, perhaps suggesting that the flux through fatty acid degradation pathways is increased when nitrogen growth limitation is relieved. L-leucine, the only acidic aliphatic amino acid investigated, responded to carbon substrate competitor additions differently from the basic non-polar amino acids L-lysine and L-arginine. For example, L-leucine uptake was enhanced in the presence of all three carbohydrates and hexanoic acid.

4. Conclusions

Pairwise comparisons of uptake kinetics and competition experiments in natural seawater incubations are challenging to interpret; however, by comparing substrates spanning a wide range of thermodynamic and chemical properties, we identified three emergent patterns of substrate selection in surface microbial communities. First, amino acids were preferentially utilized at ambient concentrations compared with all other substrates, and the number of nitrogen atoms was important to amino acid uptake kinetics. Amino acids inhibited the uptake of other amino acids, suggesting a broad specificity transporter system. Second, a linear relationship between v_o and a_p^o was identified, suggesting that interactions between transporter binding efficiency and translation among complex communities have evolved to optimize the consumption of specific substrates. Third, among the non-amino acid substrates, oxidized substrates turn over faster than reduced substrates, consistent with theoretical assimilation efficiencies. The turnover times of organic carbon substrates should therefore proceed in the order of oxidation state (alkanes > alcohols, ethers, alkenes > ketones, aldehydes, epoxides > carboxylic acids, hydroxy acids). Our results reveal that microbes are indeed picky eaters and that the surface microbial community prefers a “high protein, low calorie” diet.

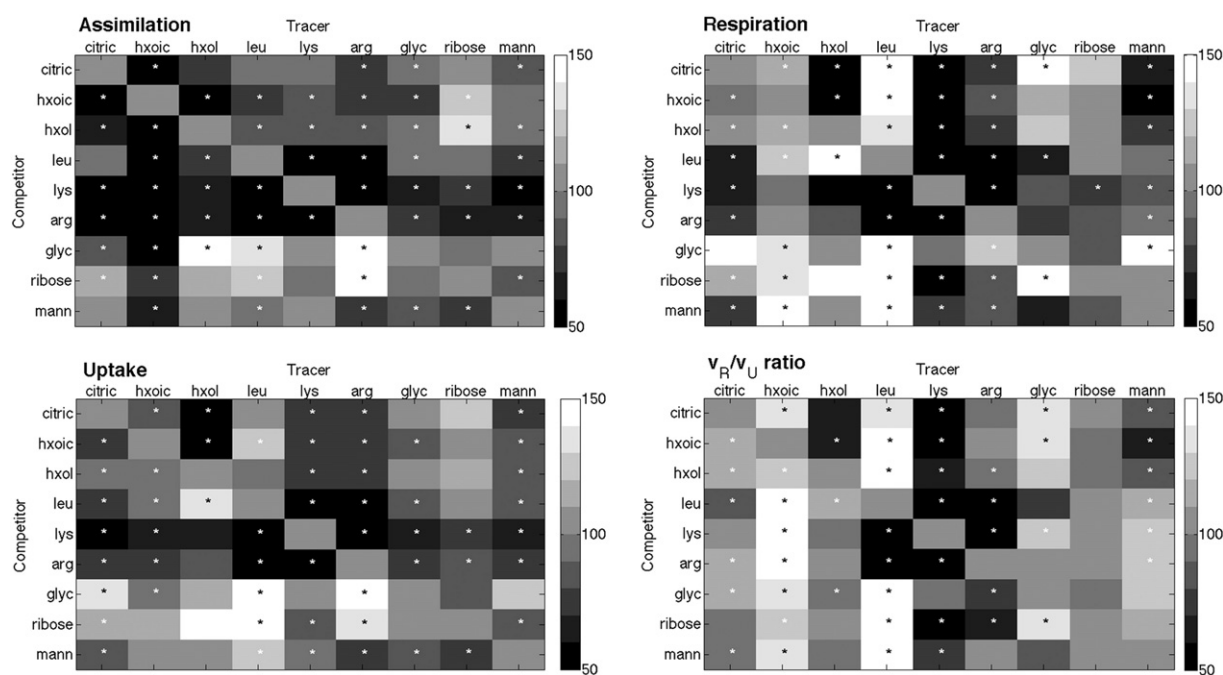


Fig. 6. Summary of competition experiments. Colors represent relative % change compared to control (the diagonal is defined as unity, 100%). Asterisks represent significant differences from the control ($p < 0.05$; Student's t -test). Substrate names are abbreviated: *cit* – citric acid, *hxoic* – hexanoic acid, *hxol* – 1-hexanol, *leu* – L-leucine, *lys* – L-lysine, *arg* – L-arginine, *glyc* – glyceraldehyde, *ribose* – D-ribose, *mann* – D-mannose.

Acknowledgments

We thank the Center for Microbial Oceanography: Research and Education (C-MORE) staff and crew of the R/V Kilo Moana for essential contributions to sample collection. We especially thank Sara Ferrón and Sandra Martínez-García for community respiration data. This work was supported by the National Science Foundation (grant EF0424599) and the Gordon and Betty Moore Foundation's Marine Microbiology Initiative (grant #3794).

References

- Albe, K.R., Butler, M.H., Wright, B.E., 1990. Cellular concentrations of enzymes and their substrates. *J. Theor. Biol.* 143, 163–195.
- Ayo, B., Unanue, M., Azua, I., Gorsky, G., Turley, C., Iriberrí, J., 2001. Kinetics of glucose and amino acid uptake by attached and free-living marine bacteria in oligotrophic waters. *Mar. Biol.* 138, 1071–1076.
- Azam, F., Hodson, R.E., 1981. Multiphasic kinetics for D-glucose uptake by assemblages of natural marine bacteria. *Mar. Ecol. Prog. Ser.* 6, 13–22.
- Bennett, B.D., Kimball, E.H., Gao, M., Osterhout, R., Van Dien, S.J., Rabinowitz, J.D., 2009. Absolute metabolite concentrations and implied enzyme active site occupancy in *Escherichia coli*. *Nat. Methods* 5, 593–599.
- Björkman, K.M., Karl, D., 2005. Presence of dissolved nucleotides in the North Pacific Subtropical Gyre and their role in cycling of dissolved organic phosphorus. *Aquat. Microb. Ecol.* 39, 193–203.
- Bunte, C., Simon, M., 1999. Bacterioplankton turnover of dissolved free monosaccharides in a mesotrophic lake. *Limnol. Oceanogr.* 44, 1862–1870.
- Button, D.K., 1993. Nutrient-limited microbial growth kinetics: overview and recent advances. *Antonie Van Leeuwenhoek* 63, 225–235.
- Carlucci, A.F., Craven, D.B., Henrichs, S.M., 1984. Diel production and microheterotrophic utilization of dissolved free amino acids in waters off Southern California. *Appl. Environ. Microbiol.* 48, 165–170.
- Casey, J., Lomas, M.W., Michelou, V., Dyhrman, S., Orchard, E., Ammerman, J.W., Sylvan, J., 2009. Phytoplankton taxon-specific orthophosphate (P_i) and ATP utilization in the western subtropical North Atlantic. *Aquat. Microb. Ecol.* 58, 31–44.
- Church, M.J., Ducklow, H.W., Karl, D., 2004. Light dependence of [³H]Leucine incorporation in the oligotrophic North Pacific Ocean. *Appl. Environ. Microbiol.* 70, 4079–4087.
- Dixon, J.L., Beale, R., Nightingale, P.D., 2011. Microbial methanol uptake in northeast Atlantic waters. *ISME J.* 5, 704–716.
- Dixon, J.L., Beale, R., Nightingale, P.D., 2013. Production of methanol, acetaldehyde, and acetone in the Atlantic Ocean. *Geophys. Res. Lett.* 40, 4700–4705.
- Donachie, S., Christian, J., Karl, D., 2001. Nutrient regulation of bacterial production and ectoenzyme activities in the subtropical North Pacific Ocean. *Deep-Sea Res. II Top. Stud. Oceanogr.* 48, 1719–1732.
- Ferguson, R.L., Sunda, W.G., 1984. Utilization of amino acids by planktonic marine bacteria: importance of clean technique and low substrate additions. *Limnol. Oceanogr.* 29, 258–274.
- Ferrón, S., Wilson, S.T., Martínez-García, S., Quay, P.D., Karl, D.M., 2015. Metabolic balance in the mixed layer of the oligotrophic North Pacific Ocean from diel changes in O₂/Ar saturation ratios. *Geophys. Res. Lett.* 42, 3421–3430.
- Fitzwater, S.E., Knauer, G.A., Martin, J.H., 1982. Metal contamination and its effect on primary production measurements. *Limnol. Oceanogr.* 27, 544–551.
- Hamilton, R.D., Austin, K.E., 1967. Assay of relative heterotrophic potential in the sea: the use of specifically labeled glucose. *Can. J. Microbiol.* 13, 1165–1173.
- Jones, R.D., 1991. Carbon monoxide and methane distribution and consumption in the photic zone of the Sargasso Sea. *Deep Sea Res. Part A* 38, 625–635.
- Karl, D., Bailiff, M., 1989. The measurement and distribution of dissolved nucleic acids in aquatic environments. *Limnol. Oceanogr.* 34, 543–558.
- Kharasch, M.S., 1929. Heats of combustion of organic compounds. *Bur. Stan. J. Res.* 2, 359–430.
- Kieber, D.J., McDaniel, J., Mopper, K., 1989. Photochemical source of biological substrates in sea water: Implications for carbon cycling. *Nature* 341, 637–639.
- King, G.M., Berman, T., 1984. Potential effects of isotopic dilution on apparent respiration in ¹⁴C heterotrophy experiments. *Mar. Ecol. Prog. Ser.* 19, 175–180.
- Kirchman, D.L., Hodson, R.E., 1984. Inhibition by peptides of amino acid uptake by bacterial populations in natural waters: implications for the regulation of amino acid transport and incorporation. *Appl. Environ. Microbiol.* 47, 624–631.
- Kirchman, D.L., Hodson, R.E., 1986. Metabolic regulation of amino acid uptake in marine waters. *Limnol. Oceanogr.* 31, 339–350.
- Logan, B.E., Fleury, R.C., 1993. Multiphasic kinetics can be an artifact of the assumption of saturable kinetics for microorganisms. *Mar. Ecol. Prog. Ser.* 102, 115–124.
- Martínez-García, S., Fernández, E., Aranguren-Gassis, M., Teira, E., 2009. In vivo electron transport system activity: a method to estimate respiration in natural marine microbial planktonic communities. *Limnol. Oceanogr. Methods* 7, 459–469.
- Mopper, K., Kieber, D.J., 1991. Distribution and biological turnover of dissolved organic compounds in the water column of the Black Sea. *Deep Sea Res. Part A* 38, 1021–1047.
- Mopper, K., Dawson, R., Liebezeit, G., Ittekkot, V., 1980. The monosaccharide spectra of natural waters. *Mar. Chem.* 10, 55–66.
- Nissen, P., Nissen, Ø., 1983. Validity of the concept of ion absorption in plants. *Physiol. Plant.* 57, 47–56.
- Nissen, H., Nissen, P., Farooq, A., 1984. Multiphasic uptake of D-glucose by an oligotrophic marine bacterium. *Mar. Ecol. Prog. Ser.* 16, 155–160.
- Poretsky, R.S., Sun, S., Mou, X., Moran, M.A., 2010. Transporter genes expressed by coastal bacterioplankton in response to dissolved organic carbon. *Environ. Microbiol.* 12, 616–627.
- Sakugawa, H., Handa, N., 1983. Chemical studies of dissolved carbohydrates in seawater. *J. Oceanogr. Soc. Jpn* 39, 279–288.
- Sun, J., Steindler, L., Thrash, J.C., Halsey, K.H., Smith, D.P., Carter, A.E., Landry, Z.C., Giovannoni, S.J., 2011. One carbon metabolism in SAR11 pelagic marine bacteria. *PLoS ONE* 6, e23973.
- Unanue, M., Ayo, B., Agis, M., Slezak, D., Herndl, G.J., Iriberrí, J., 1999. Ecto-enzymatic activity and uptake of monomers in marine bacterioplankton described by a biphasic kinetic model. *Microb. Ecol.* 37, 36–48.
- Vallino, J., Hopkinson, C.S., Hobbie, J.E., 1996. Modeling bacterial utilization of dissolved organic matter: optimization replaces Monod growth kinetics. *Limnol. Oceanogr.* 41, 1591–1609.
- Watanabe, S., Higashitani, N., Tsurushima, N., Tsunogai, S., 1995. Methane in the western North Pacific. *J. Oceanogr.* 51, 39–60.
- Westerhoff, H.V., 1993. Nonequilibrium thermodynamic considerations of the efficiency, control, and regulation of microbial growth. *Pure Appl. Chem.* 65, 1899–1906.
- Westerhoff, H.V., Hellingwerf, K.J., Van Dam, K., 1983. Thermodynamic efficiency of microbial growth is low but optimal for maximal growth rate. *Proc. Natl. Acad. Sci. U. S. A.* 80, 305–309.
- Williams, P.J.leB., 1970. Heterotrophic utilization of dissolved organic compounds in the sea I. Size distribution of population and relationship between respiration and incorporation of growth substrates. *J. Mar. Biol. Assoc. U. K.* 50, 859–870.
- Williams, P.J.leB., Yentsch, C.S., 1976. An examination of photosynthetic production, excretion of photosynthetic products, and heterotrophic utilization of dissolved organic compounds with reference to results from a coastal subtropical sea. *Mar. Biol.* 35, 31–40.
- Wright, R.R., Hobbie, J.E., 1966. Use of glucose and acetate by bacteria and algae in aquatic ecosystems. *Ecology* 47, 447–464.
- Zhou, X., Mopper, K., 1997. Photochemical production of low-molecular-weight carbonyl compounds in seawater and surface microlayer and their air-sea exchange. *Mar. Chem.* 56, 201–213.